Pharm Res (2015) 32:1055–1071
DOI 10.1007/s11095-014-1518-9

RESEARCH PAPER

Effect of Ultra-High Pressure Homogenization on the Interaction Between Bovine Casein Micelles and Ritonavir

M. Corzo-Martínez • M. Mohan • J. Dunlap • F. Harte

Received: 7 May 2014 / Accepted: 12 September 2014 / Published online: 1 October 2014
© Springer Science+Business Media New York 2014

ABSTRACT

Purpose The aim of this work was to develop a milk-based powder formulation appropriate for pediatric delivery of ritonavir (RIT).

Methods Ultra-high pressure homogenization (UHPH) at 0.1, 300 and 500 MPa was used to process a dispersion of pasteurized skim milk (SM) and ritonavir. Loading efficiency was determined by RP-HPLC-UV; characterization of RIT:SM systems was carried out by apparent average hydrodynamic diameter and rheological measurements as well as different analytical techniques including Trp fluorescence, UV spectroscopy, DSC, FTIR and SEM; and delivery capacity of casein micelles was determined by *in vitro* experiments promoting ritonavir release.

Results Ritonavir interacted efficiently with milk proteins, especially, casein micelles, regardless of the processing pressure; however, results suggest that, at 0.1 MPa, ritonavir interacts with caseins at the micellar surface, whilst, at 300 and 500 MPa, ritonavir is integrated to the protein matrix during UHPH treatment. Likewise, *in vitro* experiments showed that ritonavir release from micellar casein systems is pH dependent; with a high retention of ritonavir during simulated gastric digestion and a rapid delivery under conditions simulating the small intestine environment.

Conclusions Skim milk powder, especially, casein micelles are potentially suitable and efficient carrier systems to develop novel milk-based and low-ethanol powder formulations of ritonavir appropriate for pediatric applications.

M. Corzo-Martínez • M. Mohan
Department of Food Science and Technology, The University of Tennessee 2605 River Dr. Knoxville, Tennessee 37996-4539, USA

J. Dunlap
Division of Biology, The University of Tennessee 1414 West Cumberland Ave. Knoxville, Tennessee, 37996-0830, USA

F. Harte (✉)
Department of Food Science, Pennsylvania State University
331 Rodney A. Erickson Food Science Building
University Park, Pennsylvania 16802, USA
e-mail: fmh14@psu.edu

KEY WORDS carrier system · casein micelle · drug delivery · ritonavir · ultra-high pressure homogenization

INTRODUCTION

According to the World Health Organization (W.H.O) (1), an estimated 3.4 million children were living with HIV/AIDS at the end of 2011, 91% of them in resource-limited countries from sub-Saharan Africa where efficacious antiretroviral (ARV) treatments are still not widely accessible or available. In 2011, only 28% among affected children received an ARV treatment. According to the last revision of consolidated guidelines on the use of antiretroviral drugs for treating and preventing HIV infection carried out by W.H.O (1), the basic principles that guide the treatment of pediatric HIV infection are the same as for HIV-infected adults, due to the lack of appropriate pediatric ARV formulations and treatments. This is the case of ritonavir (RIT), an ARV drug developed by Abbott Laboratories (Table I) approved by the U.S. Food and Drug Administration (FDA) in October 3, 2005 for patients over 1 month in age (2). Ritonavir (RIT) (Table I) (3) is a potent HIV protease inhibitor (4) that is frequently prescribed in combination with other ARV agents (e.g., lopinavir, indinavir, and amprenavir) for the treatment of HIV-1 infections. RIT inhibits the cytochrome P450 3A (CYP3A)-mediated metabolism, resulting in increases ARV plasma levels and thus better efficacy (5). Despite its potent ARV effect, RIT has undesirable side effects and important oral delivery problems due to its physicochemical properties challenging its administration to infants. Among them, the most important is its high hydrophobicity and low solubility in water (Table I) which lead to low dissolution rate in the gastrointestinal fluid and, hence, to insufficient bioavailability. The liquid formulation used in infants over 1 month contains 43% ethanol and was also described as having an "awful" flavor (bitter-metallic, medicinal, astringent, sour, and burning). Moreover, in

Table I Structure and Physicochemical Properties of Ritonavir (S_w is Solubility in Water at pH 6.8 for Form I; LogD is the Distribution Coefficient at pH 6.8; and Log K_{ow} is the Coefficient of Partition in Octanol/Water)

Chemical	Commercial name [a]	Molecular weight	S_w [b]	LogD [c]	Log K_{ow} [c]
(5S,8S,10S,11S)-10-hydroxy-2-methyl-5-(1-methylethyl)-1-[2-(1-methylethyl)-4-thiazolyl]-3,6-dioxo-8,11-bis (phenylmethyl)-2,4,7,12-etraazatridecan-13-oic acid 5-thiazolyl methyl ester 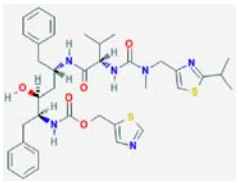	Norvir™ Soft gelatin capsules (100 mg Rit/cap) Liquid formulation (80 mg Rit/mL) KALETRA oral solution 80 mg Lopinavir + 20 mg Ritonavir/mL	720.9 g/mol	1 μg/mL	4.3	4.94

contact with the stomach mucosa, ritonavir causes nausea, vomiting, and diarrhea (3). Therefore, identifying strategies for alternative pediatric formulations of RIT and overcoming its poor aqueous solubility is needed to facilitate its oral administration to infants and children.

Over the past decade the use of naturally occurring biodegradable polymers for controlled and sustained release delivery of many drugs has increased dramatically as an alternative to synthetic polymers (6). Among these, considerable interest in recent years has been shown in the use of carrier systems based on food proteins because they are comparatively inexpensive, widely available, non-toxic (Generally Recognized As Safe, GRAS), biodegradable, and have nutritional value and good sensory properties (7). Commonly used natural food proteins include albumin and gelatin (8); however, although this topic has recently retained attention, there is limited research regarding the use of milk proteins (e.g., whey protein and caseins).

Caseins in bovine milk are amphiphilic proteins with various degrees of glycosylation and phosphorylation. The main casein proteins (α_{s1}-, α_{s2}-, β-, and κ-casein; molar ratio 4:1:4:1.3) naturally self-assemble, along with calcium phosphate nanoclusters, into highly stable micellar structures (9). Milk casein micelles are nano-delivery systems for amino acids and calcium phosphates for neonates. Although the actual structure of the casein micelle is still under discussion, its structure has been described as a block-copolymer where α_{s1}-, α_{s2}-, and β- caseins are held together by hydrophobic interactions, hydrogen bonds, and the bridging of calcium phosphate nanoclusters (10) forming a hydrophobic core. This core is surrounded by charged and diffuse surface layer attributed to κ-casein, which stabilizes the micelles against coalescence by electrostatic and steric repulsion (11).

These particular structural features confer to caseins unique potential as delivery systems of hydrophobic compounds, including binding capacity of ions and small molecules, surface-active and stabilizing properties, pH-responsive behavior, and shielding capability against radiation (12). In this regard, a number of works have demonstrated the natural tendency of individual caseins or casein micelles to bind bioactive compounds such as vitamin D (13), the flavor compound 2-nonanone (14), anticancer drugs such as mitoxantrone (15), curcumin (16), docosahexaenoic acid (DHA) (17), tea catechins (18) and β-carotene (19).

The mechanical modification of casein micelles to enhance their spontaneous tendency to bind hydrophobic compounds is attracting considerable attention. The exposure of hydrophobic residues of the individual casein proteins during homogenization at *ca.* 300 MPa and micellar reassociation has shown to be an efficient method for the binding of hydrophobic compounds such as curcumin (20), triclosan (21), and α-tocopherol acetate (7). However, to the best of our knowledge, no studies on the effect of homogenization pressures higher than 400 MPa on the loading capacity of casein micelles were reported. In the present study, we studied the effectiveness of water jet technology able to reach 500 MPa to process a dispersion of pasteurized skim milk, ritonavir, and ethanol followed by a freeze-drying for ethanol evaporation, with the purpose of developing a milk-based powder formulation appropriate for pediatric delivery of ritonavir. The use of skim milk powder as a carrier and the combination of the UHPH and freeze-drying constitutes a novel approach for drug delivery using micellar protein structures.

MATERIALS AND METHODS

Milk Source and Hydrophobic Probe

Commercial pasteurized skim milk (SM) was purchased from a local grocery store. Ritonavir (phase IIA) (RIT) was donated by Abbott Laboratories (North Chicago, IL, USA) and used as the hydrophobic probe for binding and release experiments. All other reagents were of HPLC or analytical grade.

Preparation of Ritonavir-Casein Micellar Systems

Dispersions of 0.4% RIT and SM were prepared by ultra-high pressure homogenization using a combination of Water jet technology and freeze-drying. RIT was initially dissolved in ethanol (28.6 mg RIT/ mL ethanol; Acros Organics, New Jersey, USA) under continuous agitation at 4°C until its complete dispersion. Then, RIT solution was slowly added to the skim milk under continuous agitation at room temperature to a final 14% (v/v) ethanol and 0.4% (w/v) RIT concentration. Immediately after that, 500 mL-aliquot was stored as control (RIT-SM 0.1) and the remaining dispersion was homogenized at 300 and 500 MPa (RIT-SM 300 and RIT-SM 500, using a Water jet system (Hyperjet 94 kpsi, Flow Corp., Kent, WA) equipped with zirconia-based intensifier pump and a shear resistant diamond nozzle of 4 μm internal diameter. To minimize the shear-induced increase in temperature of samples, a tube in tube heat exchanger (5.1 cm inner tube diameter; 7.6 cm outer tube diameter; 122 cm length) connected to a water bath set at 2°C (Isotemp 3016D, Fisher Scientific, Pittsburgh, Pa., U.S.A.) was placed immediately after the high-pressure nozzle. At the exit of the heat exchanger, liquid samples were collected in glass flasks to a volume of approximately 500 mL which corresponds to a RIT mass of 2 g. Non-homogenized SM without RIT (SM control 0.1) and SM without RIT run through the Water jet system at 300 and 500 MPa (SM control 300 and SM control 500) were also considered as controls. Like, RIT-SM systems, SM controls were also prepared with 14% (v/v) ethanol, as this is known to affect the casein micelle structure (it can cause immediate aggregation of casein micelles). Following homogenization, all samples were frozen at -40°C and freeze-dried to remove the ethanol and obtain a milk-based, ethanol-free powder that was stored at 4°C in a vacuum desiccator until use. Not much effect was expected due to the freezing of milk to -40°C. As an additional control, powder skim milk (no subjected to UHPH) was mixed with known amounts of RIT to obtain solid mixtures (RIT-SM mixtures) with different RIT content (0.4 – 15%, *w/w*), which were analyzed immediately after their preparation.

Separation of Ritonavir Bound to Casein micelles from Free Ritonavir and Whey Proteins

Casein micelles capable to bind RIT were separated from free RIT and whey proteins by ultracentrifugation (UCF) at 100,000xg for 40 min at 20°C using an Optima^{TM} L-100 K ultracentrifuge equipped with a fixed angle titanium rotor and polycarbonate tubes (Beckman Coulter, Fullerton, Calif., U.S.A). Immediately after ultracentrifugation, supernatants (UCF supernatants) were carefully transferred into vials using glass pipettes and pellets (UCF-pellets) were freeze-dried and stored at 4°C until further analysis.

Extraction and Quantification of Ritonavir

Extraction and quantification of RIT was carried out on non-centrifuged solid dispersions (total RIT) and UCF-supernatants (free RIT). Extraction procedure of RIT was based on a two-step liquid-liquid extraction method proposed by Zhang et al. (22) and previously used in our laboratory (23). Briefly, solid dispersions, previously hydrated in distilled water at 9.38% (w/v; approximately, the solid content of skim milk plus 0.4% RIT), were mixed with acetonitrile (ACN) at a ratio of 2:1 (v/v) (ACN: sample), inducing protein precipitation. Then mixtures were vortexed and centrifuged at 12,000 xg for 15 min and then frozen at -40°C for a minimum of 6 h to further separate the remaining water soluble proteins (frozen bottom layer) from the RIT/acetonitrile rich top layer that remained unfrozen.

Identification and quantification of RIT in acetonitrile was carried out by RP-HPLC-UV. The RIT/acetonitrile liquid layer was transferred to HPLC vials and 10 μL injected to a HPLC (model 1200, Agilent Milford, MA, USA) equipped with a reverse-phase C_{18} column (150×4.6 mm, 5 μm particle size, Zorbax Eclipse, Agilent Milford, MA, USA) at 25°C. As mobile phase, 55% ACN and 45% phosphate buffer (0.67 mM monobasic ammonium phosphate in water at pH 6.9) was used in isocratic mode for 30 min at a flow rate of 0.5 mL/min. Detection was monitored at 210 nm. Calibration was performed by using known concentrations of pure ritonavir (AP16, Abbott Park, USA), ranging from 0.05 to 2 mg/mL, diluted in skim milk and subjected to the same extraction process than samples. Calibration curves exhibited linearity (R^2>0.99) throughout the course of the study.

Ritonavir extractions were carried out in duplicate and each sample was also analyzed by duplicate (n=4) for RIT quantification by RP-HPLC-UV.

Determination of Loading Efficiency

The efficiency of the UHPH method for loading of RIT in casein micelles and the percent of unassociated, or free RIT, were calculated by Eq (1) and Eq (2), respectively:

$$\mathrm{LE\%} = [(\mathrm{RIT_{total}}–\mathrm{RIT_{free}})/\mathrm{RIT_{total}}] \times 100 \quad (1)$$

$$\%\mathrm{Unassociated\ RIT} = (\mathrm{RIT_{free}}/\mathrm{RIT_{total}}) \times 100 \quad (2)$$

Where LE is the loading efficiency; RIT_{free} is the concentration of RIT in UCF-supernatant and, hence, non-bound to casein micelles; and RIT_{total} is the RIT concentration in the sample before centrifugation.

All analytical determinations were performed in duplicate.

Stability of Ritonavir-Loaded Casein Micelles

Turbidity measurements were used to evaluate the physical stability of freeze-dried RIT-SM systems reconstituted in distilled water at 9.38% w/v and pH adjusted at 6.9. Samples were diluted 1:8 using 20 mM imidazole buffer and subsequently absorbance at 550 nm of each sample was recorded at room temperature (20°C ± 2°C) using an UV-Visible spectrophotometer (Evolution 201, Thermo Scientific, USA) and monitored over 5, 12, 24, 36, and 48 h. Samples were stored at 4°C and pH was controlled throughout the evaluation period. All measurements were done in duplicate.

The samples were also monitored for changes in apparent average hydrodynamic diameter and RIT content over the same storage period (48 h), this latter allowing the study of stability or capacity to remain soluble (not precipitate) and, hence, bioaccesible in the gastrointestinal tract, of RIT bound to casein in comparison to that of the free form. For that, pure RIT was dissolved at the comparable concentration (0.4%, *w/v*) in 14%*v/v* aqueous ethanol and pH adjusted at 6.9 (the same as that of RIT-SM systems) and total RIT concentration in both reconstituted RIT-SM systems and pure RIT dispersion was measured at 0, 5, 12, 24, 36 and 48 h by RP-HPLC-UV after extraction with ACN, as explained above. The soluble or residual RIT content was determined with the following Eq. (3). Measurements were conducted in duplicate.

$$\text{RIT}\ (\%) = (R_i/R_0)\text{x}\,100 \tag{3}$$

Where R_0 and R_i are the RIT concentrations at the beginning of the study ($t=0$) and a specific time point (5, 12, 24, 36 or 48 h), respectively.

Characterization of Reformed Ritonavir Loaded-Casein Micelles by Intrinsic Fluorescence

For fluorescence quenching determination, UCF-pellets from SM controls and RIT-SM systems were hydrated at 0.5 mg/mL in distilled water and adjusted to pH 6.9 before use. Ritonavir was dissolved in ethanol at a concentration of 0.1 M as a stock solution that was diluted with distilled water to 5 mM before titration. The fluorescence spectra were recorded using a spectrophotofluorometer (model RF-1501, Shimadzu Corp., Tokyo, Japan) using 10 mm path-length quartz cuvettes. The excitation wavelength was 285 nm. Both the excitation and emission slit widths were set at 10 nm. The emission spectra were recorded between 300 and 450 nm, with the background fluorescence calibrated using distilled water. All determinations were performed in duplicate.

Study of Ritonavir-Casein Micelle Interaction

Differencial Scanning Calorimetry (DSC) Assays

Thermal analysis of the dried UCF-pellets from SM controls and RIT-SM systems as well as of RIT-SM mixtures (0.4–15% RIT, w/w) was performed by using DSC (model Q2000, TA Instruments, USA) according to the method described by Sinha et al. (24) with modifications. Briefly, 7–10 mg of sample was placed in an aluminium pan (Tzero Pan, TA Instruments,, New Castle, DE, USA USA), crimped with a lid (Tzero Hermetic Lid, TA Instruments, New Castle, DE, USA) and kept in the differential scanning calorimeter unit along with a similar pan as a reference. The sample was heated at the rate of 10°C/min from the temperature range of 30–230°C. Nitrogen was used as a purge gas and flow was adjusted by keeping a constant pressure of 10-20 psi. All determinations were done in duplicate.

Fourier Transform Infrared (FT-IR) Spectroscopy

To gain more information about the interaction between casein micelles and ritonavir, FT-IR assays were carried out on the UCF-pellets of SM controls and RIT-SM systems. Briefly, FT-IR spectra of solid dispersion were obtained using a FT-IR system equipped with a germanium attenuated total reflection (ATR) accessory (Perkin Elmer Spectrum, Shelton, CT, USA). Solid sample was placed directly in the FT-IR sample holder in direct contact with the ATR crystal and IR spectra, in transmittance mode, were obtained in the spectral region 4,000 to 500 cm^{-1} using 1 cm^{-1} resolution. The FT-IR spectra were also obtained by the same method for the drug and SM controls. All determinations were done in duplicate.

Determination of the Morphology of RIT-SM Systems by Scanning Electron Microscopy (SEM)

Scanning electron micrographs were obtained to determine the morphology of RIT-SM solid dispersions. Samples, including pure RIT, pure RIT plus powdered SM (RIT-SM mixture), freeze-dried RIT-SM 0.1, 300 and 500 systems and freeze-dried RIT previously dispersed in ethanol (RIT-EtOH), were placed on the cover slides using double sticky copper tape prior to imaging. Subsequently, samples were imaged with a Zeiss Auriga FIB-SEM using a secondary electron detector (SE2). Parameters were 0.5 kV accelerating voltage and ~2–4 mm working distance. Magnifications were 300–60,000 X. The SEM images were processed using ImageJ (Ver Java 1.6.0_20, National Institutes of Health).

Apparent average Hydrodynamic Diameter Analysis of RIT-SM Systems

Apparent average hydrodynamic diameter (D_H) of UCF-pellets of samples obtained at 0.1, 300 and 500 MPa (solutions at 9.38%*w/v* in distilled water and diluted as needed for a proper analysis) was measured by photon correlation spectroscopy using a Delsa Nano C particle analyser (Beckman-Coulter, Fullertone, CA). Apparent average hydrodynamic diameter was calculated as the average of 70 autocorrelation functions (165° angle; 20 μm pin hole; 1% attenuation; >10 162 Kcps; refractive index 1.34). Measurements were carried out in duplicate. Calibration was checked using a standard provided by the manufacturer and by measuring native casein micelles from raw skim milk diluted in protein-free milk serum (pH 7.0). The term "apparent" is used because the assumption of a constant refractive index in samples processed using high pressure homogenization was challenged during these studies and slight over-estimation of hydrodynamic diameter and as well deviations in D_H distribution were expected.

Rheological Properties of RIT-SM Systems

RIT-SM 0.1, 300 and 500 freeze dried powders were re-suspended in distilled water to a final 9.38% (*w/v*) concentration for the determination of flow properties. Samples were left at room temperature (20°C ± 2°C) with intermittent stirring, to allow complete hydration. The rheological measurements were performed using a controlled stress rheometer (model AR2000, TA Instruments, New Castle, DE) equipped with a plate–plate geometry (40 mm diameter; 30 μm gap) on a Peltier plate set at 25°C. The flow curves were obtained by monitoring shear stress (τ, Pa) as a response to 0–120 s^{-1} shear strain rate ($\dot{\gamma}$, s^{-1}) ramp, with data recorded every 0.3 s during 1 min. All flow curves exhibited Newtonian behaviour according to:

$$\tau = \eta \cdot \dot{\gamma} \quad (4)$$

Where η is the Newtonian viscosity (Pa·s). All determinations were done in duplicate.

Determination of *In Vitro* Ritonavir Release

pH Triggered Release

Six grams of freeze-dried sample was dispersed in 65 mL HPLC water with a handheld homogenizer (9%, *w/v*). Reconstituted RIT-SM systems (initial pH of 6.9) were adjusted to pH 6, 5, 4.6, 4, 3, and 2 using 1 M HCl and pH 7, 8, 9, 10, 11, and 12 using 1 M KOH. The samples were magnetically stirred throughout the duration of the pH adjustment. At each target pH, five mL aliquots were removed after pH stabilized (approximately 5 min) to measure total RIT concentration and RIT serum concentration after ultracentrifugation as previously explained. All experiments and analytical determinations were done in duplicate.

In Vitro Gastrointestinal Digestion

With the aim of studying the effect of digestive enzymes on obtained casein-based RIT delivery systems, a gastrointestinal digestion model based on the method described by Moreno et al. (25) was used. This digestion model was based on *in vivo* data obtained by gastric and duodenal aspiration and from collection of effluent from ileostomy volunteers at the Institute of Food Research (Norwich, UK). The selection of the optimal digestive enzyme:substrate ratios reflecting those found in physiological conditions is a difficult task, as gastric and pancreatic secretions vary depending on genome as well as age, health status, and diet (26). The *in vitro* model reported here resembles physiological conditions, but it does not perfectly mimic what happens in the human gastrointestinal tract.

For the gastric digestion step, 422.5 mg of SM-RIT 0.1, 300 and 500 systems, equivalent to 150 mg of protein, were dissolved in 50 mL of simulated gastric fluid (SGF, 0.15 M NaCl, pH 2.5 adjusted with 1 M HCl). Then, a 0.32% (*w/v*) solution of porcine pepsin (EC 3.4.23.1, 3,300 activity units mg^{-1} of protein) in SGF was added to each sample at a 1:20 (*w/w*) ratio of enzyme to substrate, and digestion was performed in a shaking water bath at 37°C for 2 h, taking 5 mL sample aliquots at 5, 15 and 30 min. After this step, the pH was increased to 7.5 using 40 mM NH_4HCO_3 to inactivate pepsin. For the intestinal digestion, the pH was adjusted to 6.5 and a duodenal environment was simulated by adding: (i) a bile salt mixture containing equimolar quantities (0.125 M) of sodium taurocholate and glycodeoxycholic acid, (ii) 1 M $CaCl_2$, and (iii) 0.25 M Bis-Tris buffer, pH 6.5, at a final concentration of 7.4 mM, 9.2 mM and 24.7 mM, respectively. Solutions of porcine trypsin (0.05%, *w/v*, EC 3.4.21.4; type IX-S; 14,300 activity units mg^{-1} of protein) and bovine α-chymotrypsin (0.1%, w/v, EC 3.4.21.1, type I-S; 62 activity units mg^{-1} of protein) in water were then added at approximately physiological protein:trypsin:chymotrypsin ratios [1/(1/400)/(1/100), w/w]. Finally, samples were incubated at 37°C in a shaking water bath, and 5 mL aliquots were taken at 15, 30, 60, and 120 min. Trypsin and chymotrypsin were inactivated by heating at 80°C for 5 min. All aliquots, those obtained after incubation either with pepsin as with trypsin/chymotrypsin, were subjected to RIT extraction and analysis by RP-HPLC-UV for determining total RIT concentration and RIT serum concentration as explained above. All experiments and analytical determinations were done in duplicate. All reagents and enzymes were obtained from Sigma-Aldrich (St. Louis, MO, USA).

Statistical Analysis

Analysis of variance for variables total and free RIT, turbidity, apparent average hydrodynamic diameter, RIT stability and viscosity was done as completely randomized experiments with two replicates using SPSS version 17.0. Tukey's significant difference test was used to determine the statistical differences among treatment means. Differences were considered significant when $p<0.05$. Mean values are reported throughout the manuscript with coefficient of variation <10% in all cases.

RESULTS AND DISCUSSION

Ritonavir Recovery from Milk Fractions

RIT was extracted from the various samples and analyzed by RP-HPLC-UV. The response to RIT was found to be linear within the 0.5 to 2 mg/mL concentration range; the values of slope and correlation coefficient (R^2) of the obtained calibration curve were 47,276 and 0.999, respectively. As observed in Fig. 1, chromatographic profile of RIT displayed a well-defined peak (t_R = ~11 min) with a shoulder probably due to impurities in the sample. In addition, an almost undetectable protein peak from remaining protein in sample after extraction was also observed with a retention time of ~2 min, well separated from RIT peak, according to the results previously obtained by Roach et al. (23).

Calculated RIT recovery after extraction from RIT-SM 0.1, 300 and 500 systems resulted to be 100, 100 and 97%, respectively, which is translated to a mass percentage of total RIT in samples obtained at 0.1, 300 and 500 MPa of 0.4, 0.4 and 0.39%, respectively. This is comparable to the 0.4% of RIT content in the initial milk solutions before UHPH and freeze-drying, confirming the suitability of the used extraction and quantification methods and discarding any possible loss of RIT during sample processing (homogenization, ethanol evaporation by freeze-drying or centrifugation step during extraction).

Ritonavir Loading Efficiency

UHPH at 300 and 500 MPa of skim milk in the presence of ethanol followed by ethanol evaporation by freeze-drying and protein separation by ultracentrifugation, resulted in a significant reduction in the amount of RIT in the serum, as free RIT concentration dropped below 3% in both RIT-SM 300 and 500 vs. initial RIT level. For RIT-SM system not subjected to UHPH (RIT-SM 0.1), free RIT concentration was significantly higher ($p<0.05$) than at 300 and 500 MPa, but still low (5.3%), indicating that at 0.1 MPa the interaction RIT-casein micelles was also important. The loading efficiency (%LE), calculated as defined in Eq. (1), resulted to be 94.7, 97.4 and 98.6% for RIT-SM 0.1, 300 and 500 systems, respectively, which indicates that more than 94% of ritonavir is interacting with casein micelles for all assayed treatments. The fact that RIT-SM 0 displayed a similar %LE (94.7%) to that of systems obtained at 300 (97.4%) and 500 MPa (98.6%)

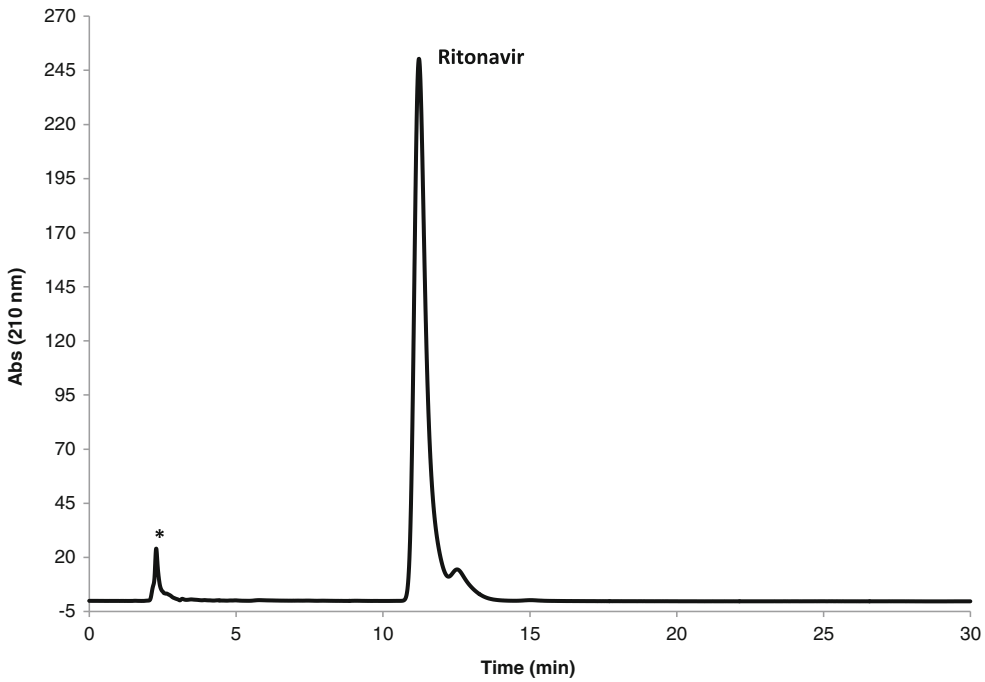

Fig. 1 HPLC chromatogram of ritonavir (RIT) recovered from skim milk. Peak marked as * corresponds to proteins that remained after the extraction process.

suggests than casein micelle spontaneously interacts with RIT when ethanol is used as co-solvent. The high %LE of RIT to casein micelles in absence of UHPH occurred only when a previous dispersion of RIT in ethanol was used. In absence of ethanol, RIT quickly precipitated and no RIT-casein interaction was evident (data not shown). In this sense, an additional study in which the drug is not previously dispersed in ethanol could result interesting to really understand the effect of UHPH on drug encapsulation within the casein micelle. Nowadays, this is carrying out in our lab.

Stability of Ritonavir-Casein Micellar Systems and Improvement of Ritonavir Dispersibility after Interaction with Caseins

Assessing the stability of RIT-SM systems is crucial to determine whether the formulation is stable long enough for handling and administration. Freeze dried samples re-suspended in water were kept under refrigeration for 48 h without stirring and absorbance (550 nm) and total ritonavir in supernatants were measured overtime. Table II shows turbidity measurements of reconstituted RIT-SM 0.1, 300 and 500 systems over 48 h. Samples were physically stable as turbidity barely varied over time, just a decrease of 9-13% over the 48 h being observed.

To study the dispersibility or capacity to remain soluble of RIT bound to casein in comparison to that of free RIT, total RIT concentration in reconstituted RIT-SM 0.1, 300 and 500 systems and pure RIT dispersion at 0, 5, 12, 24, 36 and 48 h was also determined. As expected, dispersion of RIT in water with low ethanol content (14% v/v ethanol in water) quickly precipitated and <7% of initial RIT content was quantified in the soluble phase after 48 h (calculated by Eq. (3)) (Table II). The poor stability of RIT was significantly improved after interaction with casein micelles, particularly in RIT-SM systems obtained at 300 and 500 MPa where 98 and 94% remaining RIT, respectively, was quantified after 48 h. These results indicate that interaction with casein micelles allows dispersion of water-insoluble RIT in aqueous phases.

Effects of UHPH and Ritonavir Loading on Structure of Casein Micelles

Changes in the emission spectra of tryptophan are used to evaluate structural changes of proteins, as these changes affect the local environment that surrounds the indole ring, causing shifts of wavelength of maximum fluorescence and fluorescence intensity. In particular, the maximum fluorescence intensity can be quenched by the added molecules, as the excited state of the indole ring can donate electrons to the neighboring molecules (11, 16).

Figure 2 shows the Trp fluorescence emission spectra of SM controls and RIT-SM systems. When excited at 285 nm, SM control 0.1 MPa exhibited the typical fluorescence emission spectrum of unheated skim milk, with a Trp emission maximum (λ_{max}) at 332 nm (11). At both 300 and 500 MPa, the Trp-fluorescence intensity (Trp-FI) increased in SM controls, and this was accompanied by a slight shift of the Trp

Table II Turbidity, Apparent Average Hydrodynamic Diameter (D_H) and RIT Dispersibility Measurements of RIT-Casein Micellar Systems (0, 300 and 500 MPa) During Storage at 4°C and pH 6.9 for 48 h

	Time (hours)					
	0	5	12	24	36	48
Turbidity (Abs 550 nm)						
RIT-SM 0 MPa	0.943 ± 0.016^{a}	0.921 ± 0.004^{a}	$0.844 \pm 0.013^{a*}$	$0.832 \pm 0.025^{a*}$	$0.830 \pm 0.013^{a*}$	$0.810 \pm 0.015^{a*}$
RIT-SM 300 MPa	0.990 ± 0.008^{b}	0.975 ± 0.008^{b}	0.965 ± 0.020^{b}	$0.936 \pm 0.008^{b*}$	$0.926 \pm 0.015^{b*}$	$0.902 \pm 0.023^{b*}$
RIT-SM 500 MPa	0.993 ± 0.069^{a}	0.997 ± 0.001^{c}	0.951 ± 0.051^{b}	$0.901 \pm 0.001^{c*}$	$0.881 \pm 0.001^{c*}$	$0.871 \pm 0.002^{c*}$
D_H (nm)						
RIT-SM 0 MPa	188.9 ± 2.15^{a}	187.5 ± 1.35^{a}	186.3 ± 3.11^{a}	186.2 ± 1.19^{a}	185.7 ± 2.03^{a}	186.0 ± 1.81^{a}
RIT-SM 300 MPa	215.6 ± 1.98^{b}	215.1 ± 0.92^{b}	214.5 ± 2.31^{b}	214.2 ± 1.82^{b}	212.8 ± 2.07^{b}	213.0 ± 1.79^{b}
RIT-SM 500 MPa	236.4 ± 3.01^{c}	236.3 ± 2.43^{c}	235.8 ± 1.88^{c}	235.5 ± 1.72^{c}	234.9 ± 1.41^{c}	235.1 ± 2.03^{c}
Total ritonavir (%)						
RIT-SM 0 MPa	99.54 ± 3.51^{a}	93.96 ± 3.35^{a}	$89.36 \pm 5.48^{a*}$	$87.65 \pm 3.22^{a*}$	$85.11 \pm 6.13^{a*}$	$84.71 \pm 1.72^{a*}$
RIT-SM 300 MPa	99.57 ± 4.36^{a}	98.27 ± 2.56^{a}	98.78 ± 3.69^{a}	98.30 ± 3.13^{b}	98.37 ± 3.46^{b}	98.05 ± 5.86^{b}
RIT-SM 500 MPa	99.52 ± 4.39^{a}	97.99 ± 3.71^{a}	97.34 ± 5.70^{a}	96.01 ± 3.47^{b}	94.16 ± 4.24^{b}	94.35 ± 6.70^{b}
Pure RIT	99.09 ± 2.27^{a}	$60.56 \pm 3.39^{b*}$	$39.27 \pm 2.39^{b*}$	$18.26 \pm 2.69^{c*}$	$10.44 \pm 0.51^{c*}$	$6.78 \pm 0.30^{c*}$

[a-c] Different case letters indicate statistically significant ($P < 0.05$) differences among treatments (0, 300 and 500 MPa) at the same period of time (statistical analysis by row)

[*] *Asterisk* indicates statistically significant ($P < 0.05$) differences with respect time = 0 h (statistical analysis by line)

emission maximum to 335 and 336 nm, respectively, which suggests a relatively increased exposure of tryptophan toward more hydrophilic surroundings. This means that caseins underwent conformational changes around the Trp residues (^{164}Trp and ^{199}Trp of α_{s1}-casein; ^{109}Trp and ^{193}Trp of α_{s2}-casein; ^{143}Trp of β-casein; and ^{76}Trp of κ-casein) due to micelle dissociation and subsequent re-aggregation during UHPH treatment (23, 27). This is in agreement with previous works, which reported that high pressure treatment could effectively modify the flexibility of casein molecules leading to an opening of micelle assemblies to aqueous solvent, which might explain the increase observed in Trp-FI. Particularly, the pressure-induced solubilization of α_{s1}- and α_{s2}-caseins, essentially located in the micelle core, suggested that high-pressure destabilized micelles including their internal structure (28).

In the case of RIT-SM 300 and 500 systems, the Trp-FI was lower than that of SM controls 300 and 500 (Fig. 2), which can be attributed to the quenching of the fluorescence signal by RIT bound to caseins. Moreover, compared to SM controls 300 and 500, a blue shift of the Trp emission maximum to a more hydrophobic environment (333 nm) was observed in RIT-SM 300 and 500 systems, probably due to the association of RIT to hydrophobic areas of the caseins. Since Trp residues are mostly located in the interior of the casein micelles, the fluorescence quenching and the blue shift suggests that during UHPH and ethanol evaporation RIT accesses the hydrophobic sites in the interior of the micelles, changing the casein conformation, as previously reported by Sahu et al. (16) in a study on curcumin-casein micelle complexation.. However, Trp fluorescence emission spectrum of RIT-SM 0.1 was similar to that of SM control 0.1 MPa, with no quenching or fluorescence shift observed. These results suggest that loading RIT at 0.1 MPa did not strongly affect the casein micelle conformation.

Interactions Between Ritonavir and Casein Micelles

Differencial Scanning Calorimetry (DSC) Assays

To study the interaction between RIT and casein micelles, DSC was performed on native ritonavir, UCF-pellets of SM controls and RIT-SM systems at 0.1, 300 and 500 MPa, and RIT-SM mixtures with different RIT content (0.4–15%, *w*/*w*). As shown in Fig. 3a, the thermogram for SM 0.1 MPa displayed a broad and smooth endothermic peak due to the evaporation of water contained in samples (~10%, *w*/*w*) from 50 to 150°C (29) and another stronger endothermic peak at 186°C, due to thermal degradation of casein, similar to that found by Elzoghby et al. (30). The characteristic peak at 186°C shifted to 189 and 195°C after treatment by UHPH at 300 (Fig. 3b) and 500 MPa (Fig. 3c), respectively, suggesting that homogenization protects casein against thermal degradation. The RIT thermogram revealed an endothermic peak at 125°C

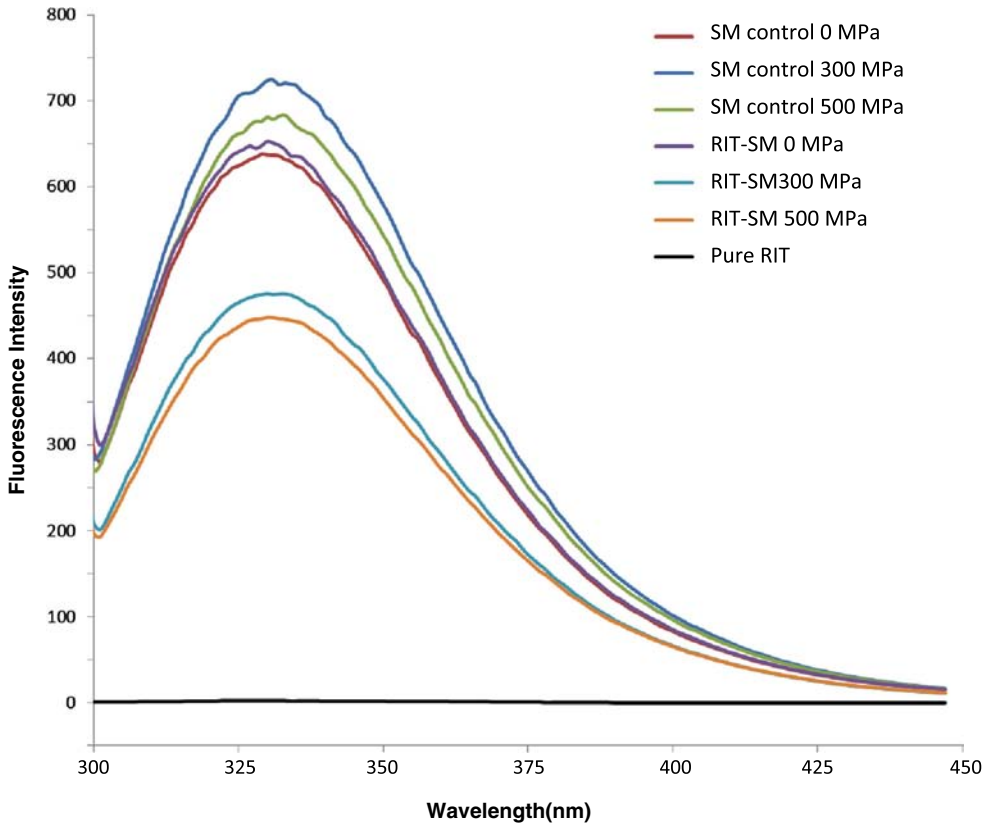

Fig. 2 Intrinsic fluorescence emission spectra of pure ritonavir (RIT) and skim milk (SM) controls and RIT-SM systems obtained at 0.1, 300 and 500 MPa.

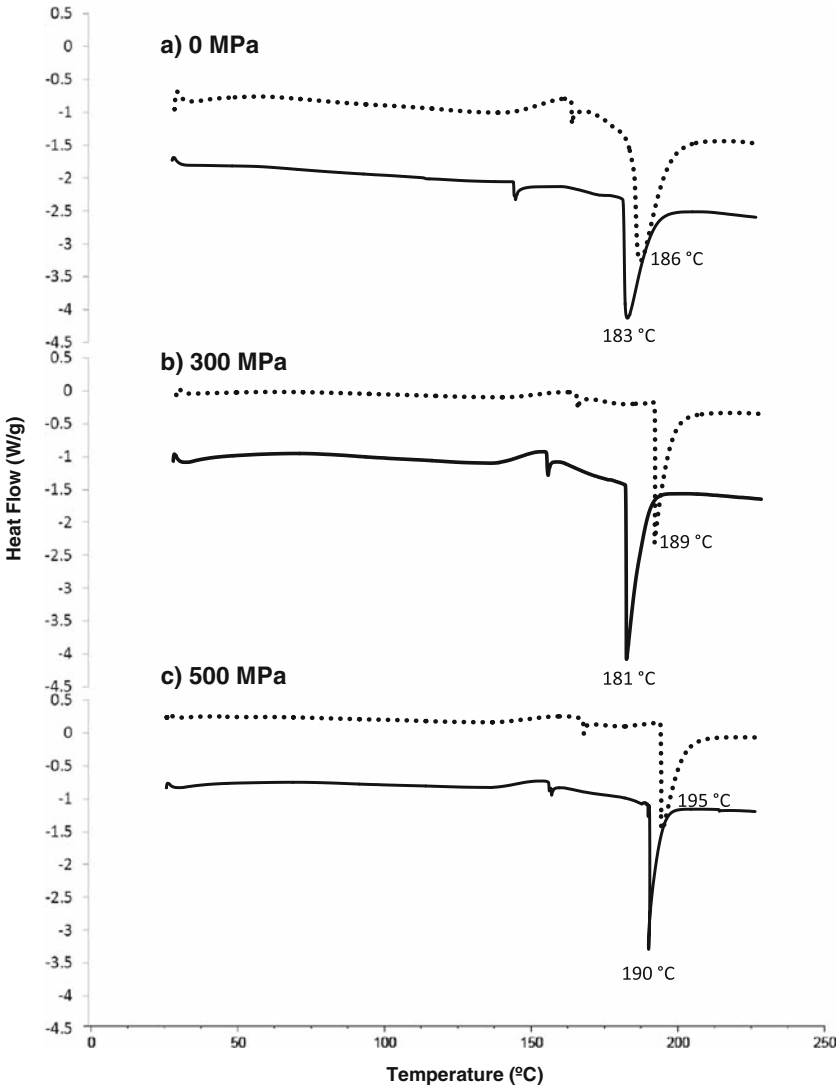

Fig. 3 DSC thermograms of skim milk (SM) controls (·····) and RIT-SM systems (—) obtained at 0.1 (**a**), 300 (**b**) and 500 (**c**) MPa.

(Fig. 4), which was attributed to the melting of RIT used in this study, confirming its form II crystalline nature in agreement with previous reports (31).

In RIT-SM mixtures, all characteristic peaks of both components (casein and RIT) were detectable, but at different melting point. So that, with decreasing RIT concentration, the drug peak was shifted to a lower melting point (~112°C) and lost its sharp and distinctive appearance, indicating a reduction of drug crystallinity (Fig. 4). Likewise, the major endothermic peak of casein was also shifted to a lower melting point with increasing RIT concentration. Thus, for 0.4% RIT, the drug concentration in homogenized systems, the RIT displayed a small but still detectable endothermic peak and casein showed a peak at 178.4°C, notably shifted with respect to the original peak at 186°C (Fig. 3a). According to results obtained by Elzoghby et al. (30) from their study on the development of a novel casein-based delivery system for flutamide, the shift of the RIT peak may be explained by presence of excess drug at micellar surface that is not completely incorporated to the micelle or may be due to physical interactions between caseins and some aggregated and amorphous state of the RIT at the micelle surface, which would also explain the shift of casein peak.

In RIT-SM 300 and 500 systems (Fig. 3b and c, respectively), no endothermic peak of RIT was observed around its original melting point. Moreover, thermograms revealed endothermic peaks corresponding to thermal degradation of casein at 181 (RIT-SM 300) and 190°C (RIT-SM 500), shifted to lower melting point with respect to those of SM 300 (189°C) and 500 (195°C). Thus, based on results from thermal analysis of RIT-SM mixtures (Fig. 4), the complete disappearance of the drug melting peak as well as the shift of casein peak observed in RIT-SM systems obtained after UHPH, especially at 300 MPa, might be attributed to the RIT integration within casein micelles in an amorphous state.

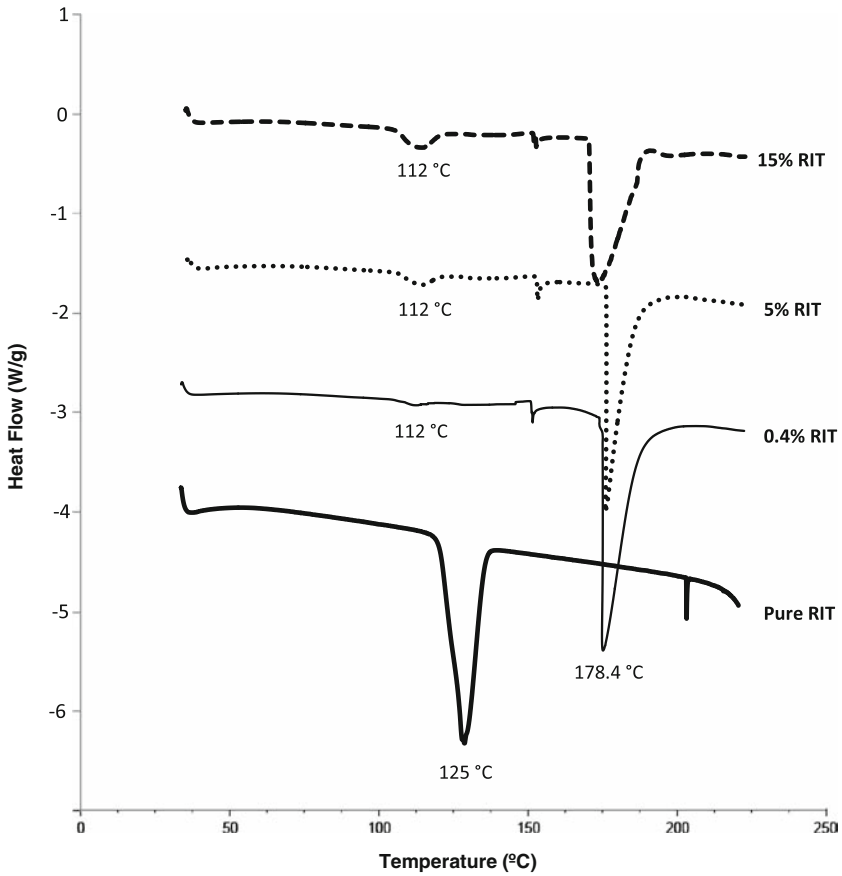

Fig. 4 DSC thermograms of pure ritonavir (RIT), non-homogenized skim milk (SM) and RIT-SM mixtures with different RIT content (0.4 – 15%, w/w).

This is supported by results previously obtained from intrinsic fluorescence (Fig. 2).

In the case of RIT-SM 0.1 system (Fig. 3a), characteristic peak of casein also appeared shifted to lower melting point (183°C) with respect to SM control 0.1 MPa (186°C), but in lesser extent than RIT-SM 300 and 500 systems. Moreover, traces of free RIT were observed in the thermogram of RIT-SM system at 0.1 MPa (results not shown), indicating that RIT present initially in the system did not totally bind to casein micelles, according to results from loading efficiency determination. This suggests that, at 0.1 MPa, association between RIT and caseins is more limited than at 300 and 500 MPa, this not being completely incorporated within the casein micelle, in agreement with results from Trp fluorescence (Fig. 2), where no changes in conformation of RIT-loaded casein micelle was observed.

FT-IR Spectroscopy

To confirm the existence of interactions between RIT and casein micelles in studied RIT-SM systems, FT-IR spectra of UCF-pellets of SM controls and RIT-SM systems were also obtained and analyzed (Fig. 5). In agreement with previous studies (30, 28), spectra of SM control 0.1 MPa showed all the normal features of a protein, with strong amide I and II peaks centering on 1,642 and 1,542 cm^{-1}, respectively, and other bands at 3455.86 and 1235.4 cm^{-1} originated also from N-H stretching and amide bending vibrations. All the strong and weak intensity bands of casein were detected in the spectra of homogenized SM controls (Fig. 5a). However, a shift in peaks corresponding to amides I and II to 1,637 and 1,546 cm^{-1}, respectively, was observed in both controls, suggesting that UHPH alters the casein conformation.

In the case of RIT-SM systems, several differences with respect to SM controls were found in terms of shift of peaks from their original position and changes in intensity. Thus, as observed in Fig. 5a for RIT-SM 300 and 500 systems, the amide II peak shifted to 1,516 and 1,525 cm^{-1}, respectively, and its intensity increased with respect to that observed in spectra of SM controls. Similarly, the peak at 1,253 cm^{-1} in SM controls 300 and 500 appeared shifted to 1,238 cm^{-1} in both RIT-SM 300 and 500 systems and with higher intensity, like peaks at 1,391 and 1,440 cm^{-1}, with higher intensity than those of SM controls, but not shifted. The peak shift and changes in band shape and slope for amides indicated the alteration of the conformation of casein micelles (29) during UHPH treatment. Non-homogenized RIT-SM system, however, just displayed a slight shift of peak corresponding to amide II, but not changes in intensity, suggesting that, at

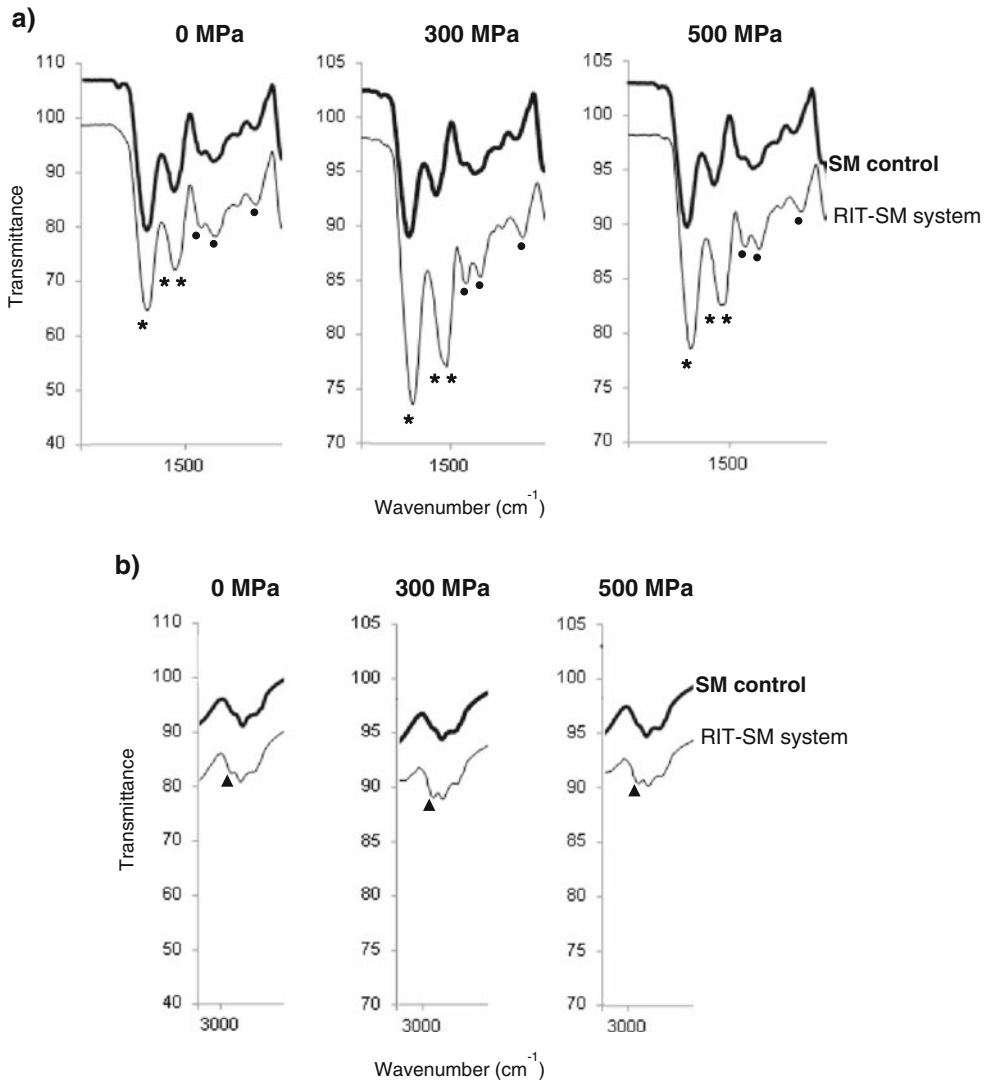

Fig. 5 FTIR spectra of SM controls () and of RIT-SM systems (—) obtained at 0, 300 and 500 MPa in the spectral region 1,600 to 1,400 cm-1 (**a**) and around 3,000 cm-1 (**b**): () Amide II; () Amide I; () N-H stretching and amide binding; () Intermolecular hydrogen bonds RIT-casein.

0.1 MPa, RIT loading does not modify notably casein conformation, according to previous results from Trp fluorescence (Fig. 2) and DSC (Fig. 3a).

Pure RIT spectrum (data not shown) displayed characteristic peaks at 3,356 cm^{-1} (N-H stretching amide group), 3,030 cm^{-1} (CH stretching), 1,716 cm^{-1} (ester linkage), and 1,645, 1,622, and 1,522 cm^{-1} (–C=C– stretching aromatic carbons) (24, 32) as well as two absorption bands at 2,870 and 2,960 cm^{-1} assigned as hydrogen bonding between ritonavir molecules, which could not be broken by aqueous fluid during dissolution resulting into low solubility (33). The characteristic peak of RIT at 2,960 cm^{-1}, not detected in spectra of SM controls, was present in spectra of all the RIT-SM systems studied, this having higher intensity in homogenized systems at 300 and 500 MPa (Fig. 5b). This indicated intermolecular hydrogen bonding formation between some of the 6/4 hydrogen acceptors/donors of RIT and some of the amino acids able to participate in hydrogen bonds of casein proteins (Gln, Asn, His, Ser, Tyr, Thr, Cys, Met, Trp) during treatment, which proves that, during UHPH treatment, RIT strongly interacts with the protein matrix, altering significantly the conformation of casein micelles. Moreover, this intermolecular hydrogen bonding formation could also be related to the higher dispersibility and stability in aqueous solutions of RIT bound to casein micelles (34).

To further study the nature of interaction between RIT and casein micelles and confirm previous results, pure RIT, RIT-SM mixture, RIT-SM 0.1, 300 and 500 systems and a control consisting in freeze-dried RIT previously dispersed in ethanol (RIT-EtOH) were analyzed by SEM. Moreover, determination of the apparent average hydrodynamic diameter and rheology of RIT-loaded casein micelles was carried out.

Determination of the Morphology of RIT-SM Systems by SEM

Figure 6a shows SEM micrograph of pure RIT crystals which displayed a similar morphology to that previously reported in

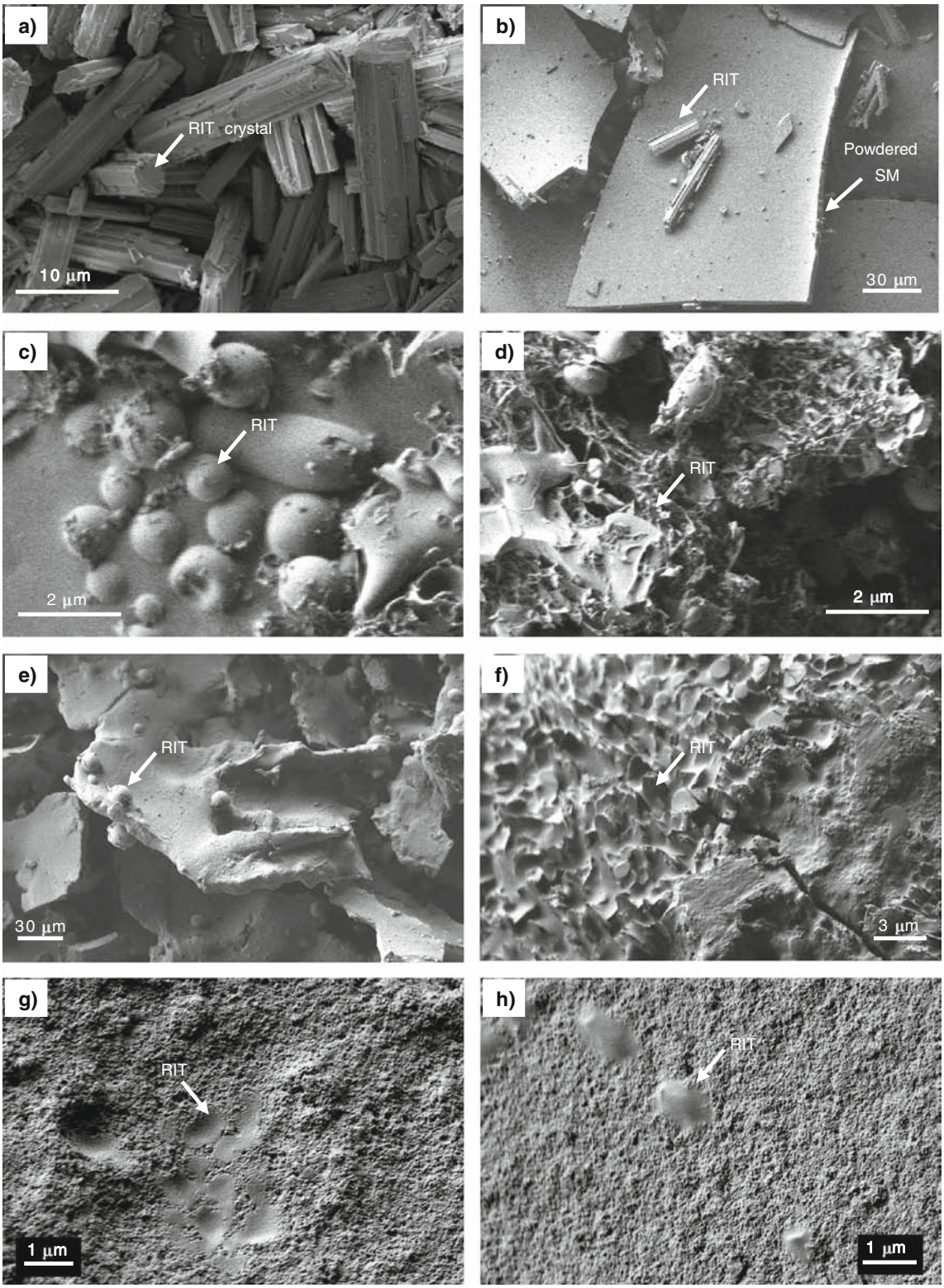

Fig. 6 SEM micrographs of pure RIT (**a**), RIT plus powdered SM (RIT-SM mixture) (**b**), freeze-dried RIT previously dispersed in ethanol (RIT-EtOH) (**c** and **d**) and freeze-dried RIT-SM 0.1 (**e** and **f**), 300 (**g**) and 500 (**h**) systems.

the literature (35). Such crystalline structure was also observed in the case of the solid mixture formed by RIT and powdered SM (RIT-SM mixture) (Fig. 6b). However, dispersion of RIT in ethanol and subsequent freezing and freeze-drying (RIT-

EtOH) gave rise to an aggregated and amorphous state of RIT as showed the SEM micrographs in Fig. 6c and d.

Figure 6e-h show the SEM micrographs obtained for freeze-dried RIT-SM 0.1, 300 and 500 systems. As expected, in the three systems, RIT showed an amorphous state similar to that observed in RIT-EtOH. However, differences regarding its interaction with the protein matrix were observed. As it is clearly observed in Fig. 6e and f, at 0.1 MPa, RIT is interacting with the surface of the protein matrix. However, at 300 and 500 MPa (Fig. 6g and h, respectively), RIT was found more embedded or integrated into the matrix, but not on the surface, demonstrating that RIT strongly interacts with the casein network, in agreement with results from DSC and FT-IR.

Determination of the Apparent Average Hydrodynamic Diameter of RIT-Loaded Casein Micelles

Table II shows results obtained after apparent average hydrodynamic diameter analysis by photon correlation spectroscopy. As observed, at time 0 (measurement just after hydrating in distilled water the RIT-SM 0.1, 300 and 500 systems), apparent average hydrodynamic diameter of casein micelles increased with increasing pressure, by 14% at 300 MPa, and by 25% at 500 MPa. Such increase in the apparent average hydrodynamic diameter might be related to the decrease in Trp fluorescence intensity observed at 500 MPa with respect 300 MPa (Fig. 2) as a result of the masking of Trp residues. These findings were in agreement with Roach et al. (23) who observed an increase in the average hydrodynamic diameter of reformed casein micelles in dispersions of skim milk, triclosan and ethanol subjected to homogenization up to 300 MPa and ethanol evaporation by spray-drying. According to these authors, the increase in apparent average hydrodynamic diameter was due to the extensive dissociation of the caseins during homogenization, giving rise to smaller casein aggregates, called neo-micelles, and subsequent re-aggregation of the neo-micelles in the homogenization valve due to: i) the shear-induced increase in temperature that promotes strong hydrophobic interactions among individual caseins; high pressure-induced denaturation of β-lactoglobulin and subsequent complexation with caseins; and iii) aggregation of neo-micelles due to lack of steric repulsion owing to the removal or collapse of κ-casein from the micelle surface during the UHPH treatment. Re-aggregation of caseins gives rise to a compact protein matrix, which was also observed by scanning electron micrographs of RIT-SM mixture and RIT-SM 300 and 500 systems (Fig. 6).

Rheology of RIT-Loaded casein Micelles

All samples displayed flow curves corresponding to Newtonian fluids when subjected to a shear strain rate from 0 to 120 s^{-1}. Table III shows average viscosity and coefficient of variation for the observed viscosity values. Like apparent average hydrodynamic diameter, a significant ($p<0.05$) increase in viscosity values was observed in all the RIT:SM systems studied, this being higher with increasing processing pressure. This might be highly correlated to the high-pressure-induced increase in the micelle size as a result of the compaction and aggregation of the smaller neo-micelles with themselves or β-lg. Moreover, according to Fox (36), intermolecular interactions and packing density are largely responsible for the rheological behavior of casein micelle systems, so that the increase observed in viscosity might be also attributed to the strengthening of protein-protein interactions from the rearrangement of micellar proteins during homogenization and ethanol evaporation resulting in more tightly associated proteins.

Ritonavir Release Behaviour of Casein Micelles

Two major factors governing the success of a carrier to enhance bioavailability are drug loading capacity and release behavior (37). Previous results have demonstrated that casein micelles possess a higher RIT loading capacity. Changes in pH of the gastrointestinal tract and the presence of digestive enzymes play a major role in effective delivery of orally administrated drugs (38). Thus, with the aim of evaluating the capacity of RIT-SM systems obtained by UHPH to serve as a potential oral delivery systems of ritonavir, two different experiments were carried out: i) RIT release under a wide range of pH values (from 2 to 12); and ii) RIT release during *in vitro* gastrointestinal digestion.

pH Triggered Release

The response of RIT-loaded casein micelles to environmental pH changes was studied. Figure 7 shows total RIT concentration throughout all experiment and concentration of RIT free in the serum at each pH value assayed (from 2 to 12). Total RIT concentration (amount of RIT in the entire sample prior to ultracentrifugation) remained constant until pH 9, from

Table III Viscosity and Coefficient of Variation (CV) of RIT-SM Systems Obtained at 0, 300, and 500 MPa, All Samples Freeze Dried and Re-Suspended in Water (9.38% w/v)

UHPH Treatment (MPa)	Viscosity (mPa·s)	CV (%)
0	3.15 [a]	2.24
300	4.10 [b]	3.45
500	4.35 [c]	1.63
Skim milk 0 MPa (control)	1.90 [d]	1.05

[a-c] Different case letters indicate statistically significant ($P<0.05$) differences among treatments

which a decrease in the recovery of RIT was observed probably due to RIT degradation under these strong alkali conditions as suggested by an additional peak observed at t_R = ~12 min in the HPLC profile of samples with pH > 10 (data not shown).

As observed in Fig. 7, at the natural pH of the reconstituted RIT-SM systems (pH 6.9), *ca.* 94, 97 and 98% of total amount of RIT was associated to casein micelles in systems subjected to 0.1, 300 and 500 MPa (calculated by Eq. (1)), respectively, and < 6% was found free in the serum after centrifugation (calculated by Eq. (2)). When pH was reduced from 6.9 to 4, free RIT levels were significantly reduced, the highest amount of RIT bound to micelles being observed at *ca.* pH 4.6. At this pH (pI of casein proteins) casein micelle precipitated out of solution dragging loaded RIT and negligible amounts of free RIT were found for all RIT-SM systems at this pH (Fig. 7). However, as pH was increased to 8, 9 and 10, a higher release of RIT from caseins to the milk serum was observed. This was especially constant for RIT-SM systems 0.1 MPa, with a maximum amount of free RIT of 7% at pH 10. For RIT-SM 500 system, a fast increase of the RIT release was observed from pH 7, reaching a maximum amount of free RIT of 10.14% at pH 9. And RIT-SM 300 system, unlike systems at 0.1 and 500 MPa, showed a moderated increase of RIT release with increasing pH, a maximum amount of free RIT of 2.84% being observed at pH 9. Once this maximum was reached, a decrease in free RIT content was found for all RIT-SM systems probably due to RIT degradation at these pH values, as mentioned above. Similarly, when pH was reduced to 3 and 2, RIT was released from the caseins increasing RIT free levels even more than at pH > 7.

The increase in the RIT release observed at extreme pH values is probably due to the breakdown of micellar integrity under extreme acidic and alkaline conditions leading to its dissociation to submicellar components. This is in agreement with Huppertz et al. (39) who observed alkaline disruption of the casein micelle at pH >10.0 as a result of: i) the disruption of the ionic and hydrophobic interactions, responsible for maintaining micellar integrity. As the pH increases, solubility of the calcium phosphate is reduced and ionic calcium and phosphate in the serum migrates into the micelle, so that the volume of water available to hydrate the exposed protein surfaces increases (40), favoring protein-solvent interactions more than ionic interactions of casein proteins along the phosphoserine residues and protein-protein interactions among the hydrophobic protein regions; ii) and the increase in the intermolecular repulsion due to the higher net negative charge of the casein proteins at alkaline pH. According to our results, RIT-SM 300 system showed a slower release of RIT than systems obtained at 0 and 500 MPa under alkaline conditions, suggesting that structural changes undergone by casein micelle during UHPH at 300 MPa might make it more resistant against dissociation under these conditions.

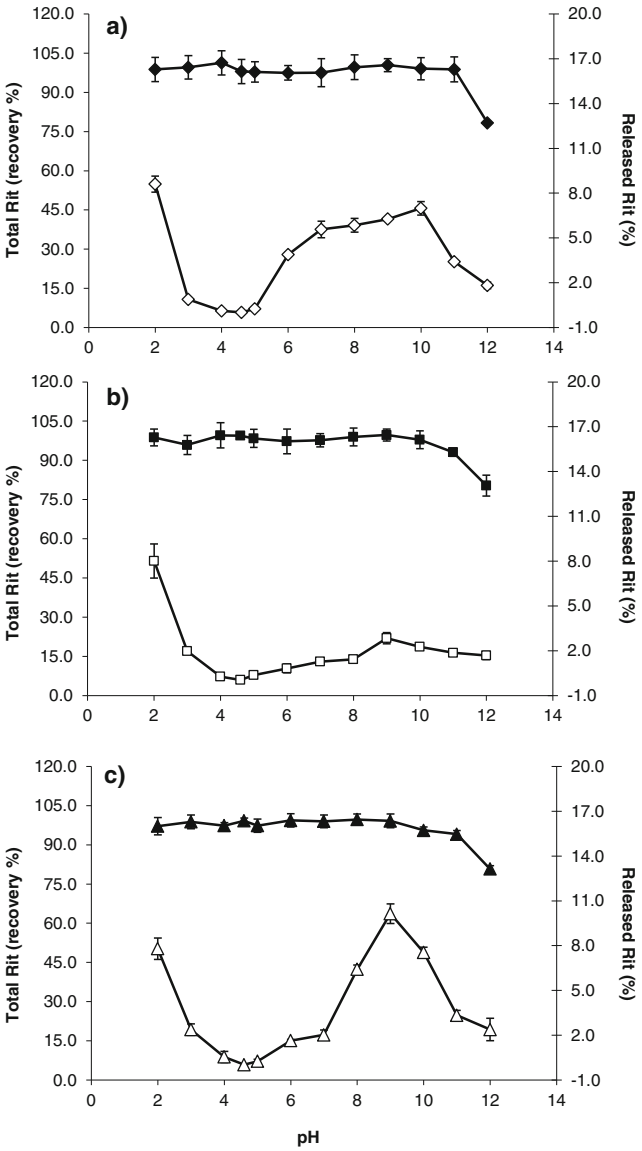

Fig. 7 Release of RIT, triggered by changes in solution pH range from 2 to 12, from loaded casein micelles of systems obtained at 0.1 (**a**), 300 (**b**) and 500 (**c**) MPa: Total RIT (solid symbols) (RIT recovered from sample at each pH with respect the initial level of RIT); Released RIT (*open symbols*) (RIT released into serum at each pH with respect total RIT). The *graphs* show means of duplicates and *error bars* represent standard deviations.

The acidic dissociation of the casein micelle at pH values below 4.0 has not been previously reported. However, it is well-known that as the pH drops below the pI, the ionization of acidic amino acids decreases whilst that of the basic amino acids increases, so that this increase in the net positive charge on the micelle might promote intermolecular repulsion leading to micellar dissociation. Moreover, during acidification, solubility of the calcium phosphate is increased, migrating from the micelle to the serum and further encouraging micelle dissociation.

In Vitro Gastrointestinal Digestion

The use of *in vitro* gastrointestinal digestion models is an economical and efficient method for screening the relative bioaccessibility of compounds in various matrices and is usually a necessary prerequisite for focused animal and human studies (41). As opposed to bioavailability (amount of drug that is absorbed, transport across the intestinal epithelia and present within blood circulation system for cellular utilization), bioaccessibility is measured as the amount of drug soluble in the intestinal tract and available for absorption, which is often the first step towards assessing bioavailability.

Thus, to study the effect of digestive enzymes on delivery capacity of the RIT-SM systems obtained by UHPH at different pressures and, thus, to know the bioaccesibility of RIT when it is ingested orally in these kind of milk-based formulations, RIT-SM 0.1, 300 and 500 systems were subjected to an *in vitro* gastrointestinal digestion model consisting of a first stage of gastric digestion with pepsin for 120 min at 37°C and a second stage of duodenal digestion with trypsin/chymotrypsin for 120 min at 37°C.

Total RIT concentration (amount of RIT in the entire sample prior to ultracentrifugation) remained constant during gastric phase; however, during duodenal phase, a decrease in recovery of total RIT was observed (Fig. 8). Tiwari and Bonde (42), in a stress study where ritonavir was subjected at 80°C for 5 h at neutral pH, observed the formation of four degradation products. Thus, it is probably that heating at 80°C for 5 min to inactivate trypsin and chymotrypsin promotes some ritonavir degradation, which might explain the decrease observed in the recovery of total ritonavir during the duodenal phase.

During gastric phase of digestion, the release of RIT in all RIT-SM systems was prevented (Fig. 8), only < 7% of the total amount of RIT being found free in UCF-supernatants. This is according to Benzaria et al. (20), who in a study on the effect of dynamic high-pressure on the interaction of curcumin with phosphocasein micelles (PC), observed that digestibility of PC–curcumin complexes were quite resistant to *in vitro* pepsin treatment. Such results indicate that casein proteins strongly retain RIT in conditions simulating the stomach environment, which might be attributed to that under acidic conditions of gastric solution casein proteins precipitate along with RIT, preventing its release. Acid-induced precipitation leads to a higher protective effect against proteolysis by pepsin, which could be explained as peptic cleavage sites (hydrophobic or aromatic amino acid side chains) are buried after aggregation and precipitation of caseins, forming a strong hydrophobic core and preventing hydrolysis.

After 2 h of gastric digestion, the pH was raised to 6.5, irreversibly inactivating pepsin and mimicking the transfer of gastric contents into the duodenal compartment. Combined trypsin/chymotrypsin digestion of RIT-SM 0.1, 300 and 500 systems in the presence of bile salts was followed for up to 120 min in the duodenal phase.

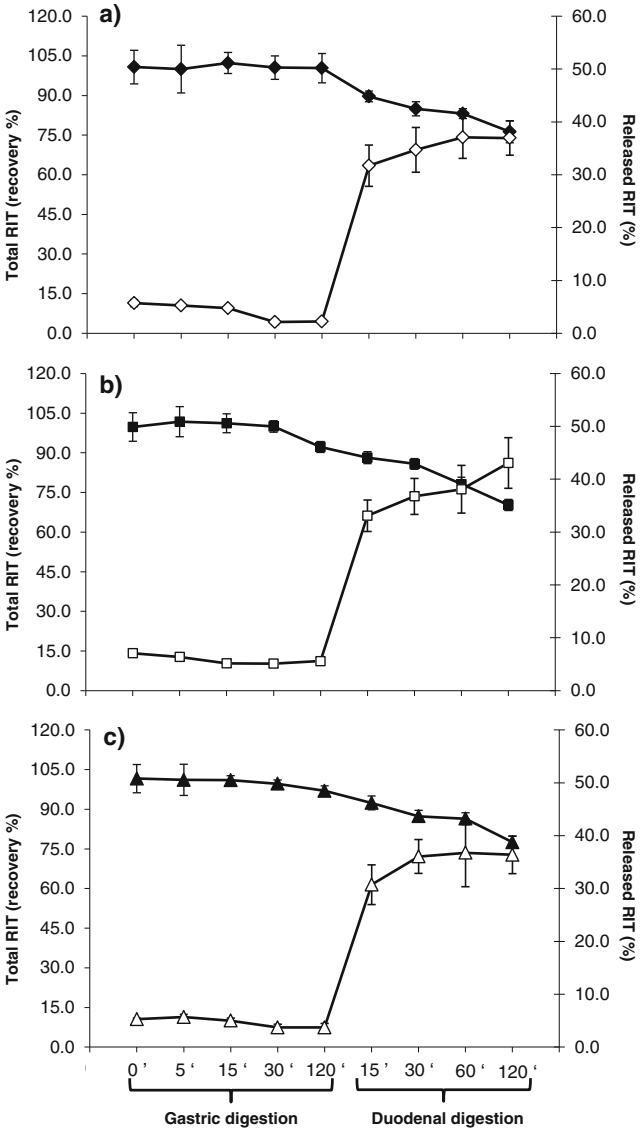

Fig. 8 Release of RIT, under conditions simulating gastrointestinal digestion (pepsin digestion for 2 h at pH 2.5 and 37°C followed by trypsin/chymotrypsin digestion for 2 h at pH 6.5 and 37°C), from loaded casein micelles of systems obtained at 0.1 (**a**), 300 (**b**) and 500 (**c**) MPa: Total RIT (solid symbols) (RIT recovered from sample at each pH with respect the initial level of RIT); Released RIT (open symbols) (RIT released into serum at each pH with respect total RIT). The *graphs* show means of duplicates and *error bars* represent standard deviations.

Conversely to the stage of gastric digestion, over 30% of the total amount of RIT was quickly released after 15 min of incubation with trypsin/chymotrypsin. After 120 min, ~ 40% of the total amount of RIT was released by casein micelles in the intestine, a slightly higher release of RIT being observed for RIT-SM 300 system (Fig. 8b). Based on the results from the pH triggered release, less than 5% of RIT was released at the equivalent pH of 6 or 7. This might be due to trypsin and

chymotrypsin activity that proteolyzes casein micelles promoting or enhancing RIT release, suggesting, along with results from pH triggered release, that casein micelle dissociation and/or casein proteolysis is necessary for the release of bound compounds, in this case RIT. This is in agreement with Benzaria et al. (20), who observed that *in vitro* pancreatin treatment caused a greater and faster curcumin release than pepsin treatment.

However, despite of the digestive enzyme effect, bioaccessibility of RIT resulted to be lower than we expected probably due to the strong interaction with casein micelles in the three studied systems.

CONCLUSIONS

Determination of loading efficiency showed that RIT interacts efficiently with casein micelles, regardless of the processing pressure, probably due to the previous dispersion of RIT in ethanol which facilitates its interaction with casein micelles. Such association significantly improved RIT stability as compared to that of free RIT in 14% aqueous ethanol.

Moreover, results showed that the nature of the RIT-casein micelle interaction is processing-dependant. So that, it can be hypothesized that, at 300 and 500 MPa, RIT is completely incorporated within the protein matrix resulting from the UHPH treatment, probably interacting with the hydrophobic regions located in the micelle core, whilst at 0 MPa, although RIT efficiently interacts with casein micelles, their association is more limited, so that drug is not integrated to the protein matrix but it mainly interacts at the surface.

In vitro experiments at different pH values and under simulated gastrointestinal conditions showed that release of RIT associated with casein micelles is pH-dependant, so that casein micelle efficiently protects associated hydrophobic compounds from degradation in the acidic environment of the stomach, as it allows bypassing the gastric environment and delivering RIT in the early portions of the small intestine. In the case of RIT, this could avoid nausea, diarrhea, and vomiting related to its direct effect on stomach.

Rate and extent of RIT absorption in the casein-based formulation is expected to be at least equivalent to that of the commercial product. However, further *in vitro* studies with Caco-2 cells and, especially, *in vivo* experiments are necessary to confirm both the effectiveness and oral bioavailability of obtained RIT-casein micellar systems. Currently, an *in vivo* study with piglets is being carried out in our lab with this purpose.

In conclusion, based on results derived from this work, we can say that casein micelles are potentially suitable and efficient carriers systems to develop cheap and easily usable milk-based and low-ethanol powder formulations of ritonavir with better physicochemical properties (water-soluble) than the current commercial product, which might allow the economic health care for children with HIV.

ACKNOWLEDGMENTS AND DISCLOSURES

Research reported in this publication was supported by the Eunice Kennedy Shriver National Institute of Child Health and Human Development of the National Institutes of Health under award number R21HD065170. The content is solely the responsibility of the authors and does not necessarily represent the official views of the National Institutes of Health. We acknowledge Abbott Laboratories for kindly donating the ritonavir used in this study.

REFERENCES

1. World Health Organization (W.H.O). Consolidated guidelines on the use of antiretroviral drugs for treating and preventing HIV infection. 2013.
2. Giaquinto C, Morelli E, Fregonese F, Rampon O, Penazzato M, de Rossi A, *et al.* Current and future antiretroviral treatment options in paediatric HIV infection. Clin Drug Investig. 2008;28(6):375–97.
3. Abbott Laboratories. Norvir (ritonavir capsules) soft gelatin/(ritonavir oral solution). North Chicago, IL. 2006. Available from: http://www.rxabbott.com/pdf/norpi2a.pdf
4. Chen XQ, Kempf DJ, Li L, Sham HL, Vasavanonda S, Wideburg NE, *et al.* Synthesis and SAR studies of potent HIV protease inhibitors containing novel dimethylphenoxyl acetates as P-2 ligands. Bioorg Med Chem Lett. 2003;13(21):3657–60.
5. Sevrioukova IF, Poulos TL. Structure and mechanism of the complex between cytochrome P4503A4 and ritonavir. Proc Natl Acad Sci. 2010;107(43):18422–7.
6. Lu Y, Chen S. Micro and nano-fabrication of biodegradable polymers for drug delivery. Adv Drug Deliv Rev. 2004;56(11):1621–33.
7. Chevalier-Lucia D, Blayo C, Gràcia-Julià A, Picart-Palmade L, Dumay E. Processing of phosphocasein dispersions by dynamic high pressure: effects on the dispersion physico-chemical characteristics and the binding of α-tocopherol acetate to casein micelles. Innov Food Sci Emerg Technol. 2011;12(4):416–25.
8. Kommareddy S, Amiji M. Preparation and evaluation of thiol-modified gelatin nanoparticles for intracellular DNA delivery in response to glutathione. Bioconjugate Chem. 2005;16(6):1423–32.
9. Braga ALM, Menossi M, Cunha RL. The effect of the glucono-delta-lactone/caseinate ratio on sodium caseinate gelation. Int Dairy J. 2006;16(5):389–98.
10. De Kruif C, Holt C. Casein micelle structure, functions and interactions. In: Fox PF, McSweeney PLH, editors. Advanced dairy chemistry—1 proteins. New York: Springer; 2003. p. 233–76.
11. Yazdi SR, Corredig M. Heating of milk alters the binding of curcumin to casein micelles. a fluorescence spectroscopy study. Food Chem. 2012;132(3):1143–9.
12. Livney YD. Milk proteins as vehicles for bioactives. Curr Opin Colloid Interf Sci. 2010;15(1):73–83.
13. Semo E, Kesselman E, Danino D, Livney YD. Casein micelle as a natural nano-capsular vehicle for nutraceuticals. Food Hydrocoll. 2007;21(5):936–42.
14. Kühn J, Zhu X-Q, Considine T, Singh H. Binding of 2-nonanone and milk proteins in aqueous model systems. J Agric Food Chem. 2007;55(9):3599–604.

15. Shapira A, Assaraf YG, Livney YD. Beta-casein nanovehicles for oral delivery of chemotherapeutic drugs. Nanomed Nanotech Biol Med. 2010;6(1):119–26.
16. Sahu A, Kasoju N, Bora U. Fluorescence study of the curcumin−casein micelle complexation and its application as a drug nanocarrier to cancer cells. Biomacromol. 2008;9(10):2905–12.
17. Zimet P, Rosenberg D, Livney YD. Re-assembled casein micelles and casein naoparticles as nano-vehicles for ω-3 polyunsaturated fatty acids. Food Hydrocoll. 2011;25:1270–6.
18. Haratigar S, Correding M. Interactions between tea catechins and casein micelles and their impact on renneting functionality. Food Chem. 2014;143:27–32.
19. Pan X, Yao P, Jiang M. Simultaneous nanoparticle formation and encapsulation driven by hydrophobic interaction of casein-*graft*-dextran and β-carotene. J Colloid Interf Sci. 2007;315(2):456–63.
20. Benzaria A, Maresca M, Taieb N, Dumay E. Interaction of curcumin with phosphocasein micelles processed or not by dynamic high-pressure. Food Chem. 2013;138:2327–37.
21. Roach A, Harte F. Disruption and sedimentation of casein micelles and casein micelle isolates under high-pressure homogenization. Innov Food Sci Emerg Technol. 2008;9(1):1–8.
22. Zhang M, Moore GA, Gardiner SJ, Begg EJ. Determination of celecoxib in human plasma and breast milk by high-performance liquid chromatographic assay. J Chromatogr B. 2006;830(2):245–8.
23. Roach A, Dunlap J, Harte F. Association of triclosan to casein proteins through solvent–mediated high–pressure homogenization. J Food Sci. 2009;74(2):N23–9.
24. Sinha S, Ali M, Baboota S, Ahuja A, Kumar A, Ali J. Solid dispersion as an approach for bioavailability enhancement of poorly water-soluble drug ritonavir. AAPS PharmSciTech. 2010;11(2):518–27.
25. Moreno FJ, Mellon FA, Wickham MS, Bottrill AR, Mills E. Stability of the major allergen Brazil nut 2S albumin (Ber e 1) to physiologically relevant in vitro gastrointestinal digestion. FEBS J. 2005;272(2):341–52.
26. Moreno FJ. Gastrointestinal digestion of food allergens: effect on their allergenicity. Biomed Pharmacother. 2007;61(1):50–60.
27. Yazdi SR. Changing the structure of casein micelles to improve the delivery of bioactive compounds. PhD Thesis. 2012.
28. Regnault S, Dumay E, Cheftel JC. Pressurisation of raw skim milk and of a dispersion of phosphocaseinate at 9°C or 20°C: effects on the distribution of minerals and proteins between colloidal and soluble phases. J Dairy Res. 2006;73(1):91–100.
29. Zhang Y, Zhong Q. Encapsulation of bixin in sodium caseinate to deliver the colorant in transparent dispersions. Food Hydrocoll. 2013;33:1–9.
30. Elzoghby AO, Helmy MW, Samy WM, Elgindy NA. Spray-dried casein-based micelles as a vehicle for solubilization and controlled delivery of flutamide: formulation, characterization, and in vivo pharmacokinetics. Eur J Pharm Biopharm. 2013;84:487–96.
31. Chemburkar SR, Bauer J, Deming K, Spiwek H, Patel K, Morris J, *et al.* Dealing with the impact of ritonavir polymorphs on the late stages of bulk drug process development. Org Process Res Dev. 2000;4(5):413–7.
32. Jenita JJL, Madhusudhan NT, Wilson B, Manjula D, Savitha BK. Formulation and characterization of ritonavir loaded ethyl cellulose microspheres for oral delivery. World J Pharm Res. 2012;1(2):207–15.
33. Poddar SS, Nigade SU, Singh DK. Designing of ritonavir solid dispersion through spray drying. Der Pharm Lett. 2011;3(5):213–23.
34. Pelton JT, McLean LR. Spectroscopic methods for analysis of protein secondary structure. Anal Biochem. 2000;277(2):167–76.
35. Ilevbare GA, Liu H, Edgar KJ, Taylor LS. Inhibition of solution crystal growth of ritonavir by cellulose polymers–factors influencing polymer effectiveness. CrystEngComm. 2012;14(20):6503–14.
36. Fox PF. Milk proteins: general and historical aspects. In: Fox PF, McSweeney PLH, editors. Advanced dairy chemistry—1 proteins. New York: Springer; 2003. p. 1–48.
37. Liu J, Lee H, Allen C. Formulation of drugs in block copolymer micelles: drug loading and release. Curr Pharm Design. 2006;12(36):4685–701.
38. Perales S, Barberá R, Lagarda MJ, Farré R. Availability of iron from milk-based formulas and fruit juices containing milk and cereals estimated by *in vitro* methods (solubility, dialysability) and uptake and transport by Caco-2 cells. Food Chem. 2007;102(4):1296–303.
39. Huppertz T, Vaia B, Smiddy MA. Reformation of casein particles from alkaline-disrupted casein micelles. J Dairy Res. 2008;75(1):44–7.
40. Vaia B, Smiddy MA, Kelly AL, Huppertz T. Solvent-mediated disruption of bovine casein micelles at alkaline pH. J Agric Food Chem. 2006;54(21):8288–93.
41. Failla ML, Huo T, Thakkar SK. In vitro screening of relative bioaccessibility of carotenoids from foods. Asia Pac J Clin Nutr. 2008;17(S1):200–3.
42. Tiwari RN, Bonde CG. LC, LC-MS/TOF and MSn studies for the separation, identification and characterization of degradation products of ritonavir. Anal Methods. 2011;3:1674–81.